Proceedings of OMAE'03
22nd International Conference on Offshore Mechanics and Arctic Engineering
June 8-13, 2003, Cancun Mexico

OMAE2003-37465

MODELLING OF SEABED INTERACTION IN FREQUENCY DOMAIN ANALYSIS OF MOORING CABLES

Paul P. A. Ong*
Department of Engineering
University of Cambridge
Cambridge CB2 1PZ
United Kingdom
Email: ppao2@cam.ac.uk

Sergio Pellegrino
Department of Engineering
University of Cambridge
Cambridge CB2 1PZ
United Kingdom
Email: sp28@cam.ac.uk

Keywords: Mooring Cables, Seabed Interaction, Frequency Domain

ABSTRACT

Mooring cables under wave loading interact dynamically with the seabed; this interaction is nonlinear and can be modelled in full only by performing lengthy time integration of the equations of motion. However, time domain integration is far too computationally expensive to be carried out for all load cases. A new method of modelling the interaction between a cable and the seabed in the frequency domain, but without considering frictional effects and impact, is therefore proposed. The section of cable interacting with the seabed is truncated and replaced with a system of coupled linear springs, with stiffnesses linearised from static catenary equations. These springs would model the behaviour of the truncated cable and hence the time-varying boundary condition at the touchdown. The entire cable-spring system is then analysed in the frequency domain with a centred finite difference scheme. The proposed method has shown to increase the accuracy of frequency domain analysis in certain cases with affordable computational overhead.

*Address all correspondence to this author.

NOMENCLATURE

AE	Axial stiffness
C_N	Normal drag coefficient
C_T	Tangential drag coefficient
F_{Dn}	Normal drag force
F_{Dt}	Tangential drag force
H	Horizontal force component
L_g	Grounded cable length
L	Total cable length
T_e	Effective tension
T_f	Mean fairlead tension
V	Vertical force component
V_c	Current flow velocity
d_0	Unstretched cable diameter
h	Water depth
k	Spring stiffness
m_0	Dry unit mass
m_a	Added unit mass
s	Arc length
u	Tangential cable velocity
v	Normal cable velocity
w	Submerged unit weight
x	Horizontal cable coordinate
z	Vertical cable coordinate
ε	Axial strain
ω	Excitation frequency
ϕ	Inclination of cable w.r.t. horizontal
ρ	Water density

INTRODUCTION

As mooring structures are becoming increasingly important to the offshore oil and gas industry, there is a continuing need to improve the designs of such structures through better prediction of their nonlinear behaviour. Many time domain codes exist to fulfil this need but many fall short of a fast prediction required for the analyses of numerous test cases.

Although more efficient and equally widely used, frequency domain analysis requires the linearisation of various nonlinear aspects of mooring cable behaviour. One such aspect is the time-varying interaction between the grounded cable and the seabed, which can only be modelled in full by performing lengthy time integration of the equations of motion.

Thus, for simplicity, some early investigators of frequency domain methods have conservatively assumed the touchdown of a cable as fixed throughout the dynamic analysis [1, 2]. While others like Kwan and Bruen [3] have replaced the grounded cable with an equivalent horizontal spring with no lift off allowed. In a comparative study carried out by Wu [4] using both methods, it was found that the spring model works well only in deep waters where a small portion of line lies on the seabed.

Both the fixed touchdown and linear spring models however restrict the grounded cable from lifting off and touching down. To model this effect, while ignoring friction on the seabed and any impact force arising from the touchdown action, Chatjigeorgiou and Mavrakos [5] computed quasi-statically the instantaneous touchdown point before solving dynamically for the suspended cable. Comparing this approach with the horizontal spring model, the latter was found to severely over-predict the working tensions whenever the excitation at the fairlead is also large.

Alternatively, liftoff and touchdown effects can be modelled in the time domain by applying an upthrust to any nodes on the cable that touches the seabed, as proposed by Ghadimi [6]. The grounded cable would appear to rest on the seabed as long as the upthrust was maintained. A similar approach, in a form of a "mattress" with distributed elastic support, was also attempted by Inoue and Surendran [7] and Webster [8]. The primary difficulty with this approach is in determining the appropriate stiffness constants for the type of soil concerned.

Depending on the speed of the touchdown point, the action of lifting off and touching down may generate large dynamic tension peaks, as pointed out by Triantafyllou et al. [9]. This effect was further validated through experiments and numerical simulations by Gobat and Grosenbaugh [10]. To prevent shocks from occurring in numerical simulations, researchers like Thomas and Hearn [11] reduced the nodal mass of any nodes approaching the seabed.

This paper introduces a new method of modelling seabed interaction which accounts for the effect of axial stretching as well as liftoff and touchdown in the frequency domain, but ignoring any frictional effects and impact between the cable and seabed. This is achieved by truncating and replacing the section of grounded cable with a system of coupled linear springs. These springs would model the behaviour of the truncated cable and hence the time-varying boundary condition at the touchdown. The paper begins by first outlining the governing equations and the formulation of a frequency domain analysis. The new method of seabed modelling will be described next, together with the linearisation process required to establish the spring stiffnesses. Finally, test solutions obtained for various cable configurations will be compared to that of time domain and conclusions drawn.

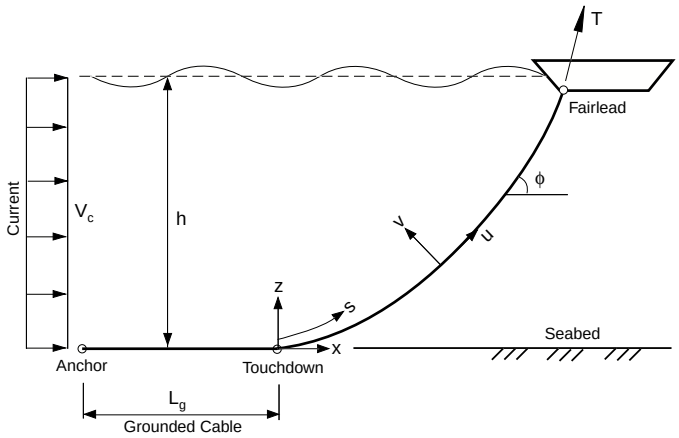

Figure 1. Schematic of mooring cable

FREQUENCY DOMAIN ANALYSIS

Governing Equations

The standard equations governing the dynamic behaviour of a general catenary mooring cable shown in Fig. 1 are [1]:

$$
\begin{aligned}
(m_0+m_a)\frac{\partial v}{\partial t}+(m_0u+m_aV_c\cos\phi)\frac{\partial \phi}{\partial t} &= T_e\frac{\partial \phi}{\partial s}-w\cos\phi-F_{Dn}\\
m_0\left(\frac{\partial u}{\partial t}-v\frac{\partial \phi}{\partial t}\right) &= \frac{\partial T_e}{\partial s}-w\sin\phi+F_{Dt}\\
\frac{\partial \varepsilon}{\partial t} &= \frac{\partial u}{\partial s}-v\frac{\partial \phi}{\partial s}\\
(1+\varepsilon)\frac{\partial \phi}{\partial t} &= \frac{\partial v}{\partial s}+u\frac{\partial \phi}{\partial s}\\
\frac{\partial z}{\partial t} &= v\cos\phi+u\sin\phi\\
\frac{\partial x}{\partial t} &= u\cos\phi-v\sin\phi
\end{aligned}
\qquad (1)
$$

For simplicity, the linear stress-strain relationship $\varepsilon = T_e/AE$ is assumed.

For the purpose of frequency domain analysis, we linearise the above equations by assuming the cable is undergoing simple harmonic motion about its static equilibrium position. Hence, we assume

$$\begin{aligned} u &= u_0 + u_1 e^{i\omega t} \\ v &= v_0 + v_1 e^{i\omega t} \\ T_e &= T_{e0} + T_{e1} e^{i\omega t} \\ \phi &= \phi_0 + \phi_1 e^{i\omega t} \end{aligned} \tag{2}$$

where subscripts 0 and 1 denote static and dynamic values respectively.

We also linearise the nonlinear Morrison's drag forces, F_{Dn} and F_{Dt}, in Eqs. (1) using the linearisation method developed by Krolikowski and Gay [12]. Equations. (1) can therefore be simplified to

$$\frac{d}{ds}\begin{bmatrix} u_1 \\ v_1 \\ T_{e1} \\ \phi_1 \end{bmatrix} = \begin{bmatrix} 0 & a_{12} & a_{13} & 0 \\ a_{21} & 0 & 0 & a_{24} \\ a_{31} & 0 & 0 & a_{34} \\ 0 & a_{42} & a_{43} & a_{44} \end{bmatrix} \begin{bmatrix} u_1 \\ v_1 \\ T_{e1} \\ \phi_1 \end{bmatrix} + \begin{bmatrix} 0 \\ 0 \\ b_{31} \\ b_{41} \end{bmatrix} \tag{3}$$

where

$$\begin{aligned} a_{12} &= \frac{d\phi_0}{ds} \\ a_{13} &= \frac{i\omega}{AE} \\ a_{21} &= -\frac{d\phi_0}{ds} \\ a_{24} &= i\omega(1+\varepsilon_0) \\ a_{31} &= i\omega m_0 + F_{Dt1} \\ a_{34} &= w\cos\phi_0 \\ a_{42} &= \left[i\omega(m_0+m_a) - F_{Dn1}\right]\frac{1}{T_{e0}} \\ a_{43} &= -\frac{d\phi_0}{ds}\frac{1}{T_{e0}} \\ a_{44} &= \left[i\omega m_a V_c \cos\phi_0 - w\sin\phi_0\right]\frac{1}{T_{e0}} \\ b_{31} &= -F_{Dt1}u_w \\ b_{41} &= \left(F_{Dn1}v_w\right)\frac{1}{T_{e0}} \end{aligned} \tag{4}$$

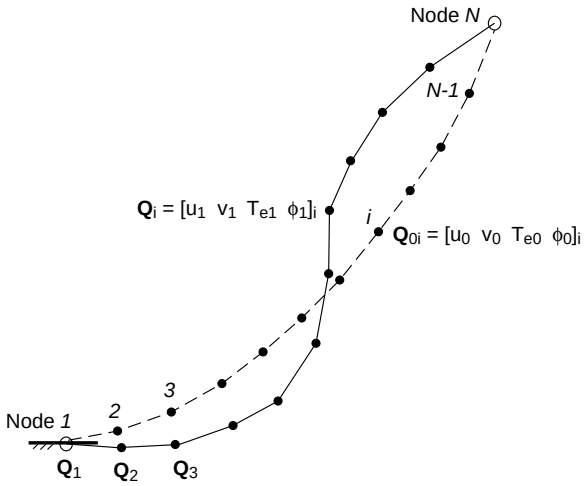

Figure 2. Schematic representation of finite difference scheme

Numerical Scheme

Equation (3) is solved using an explicit centred finite difference scheme [13]. Dividing the cable into *N-1* elements and *N* nodes, see Fig. 2, we rewrite Eq. (3) as

$$\frac{\mathbf{Q}_{i+1} - \mathbf{Q}_i}{\Delta s} = \frac{\mathbf{A}_{i+1}\mathbf{Q}_{i+1} + \mathbf{B}_{i+1} + \mathbf{A}_i\mathbf{Q}_i + \mathbf{B}_i}{2} + O(\Delta s^2) \tag{5}$$

where $\mathbf{Q} = [u_1 \;\; v_1 \;\; T_{e1} \;\; \phi_1]$, $\mathbf{A}$ and $\mathbf{B}$ denote the 4-by-4 matrix and the vector in Eq. (3) respectively, subscript i the i-th node on the cable, and $O(\Delta s^2)$ the error Δs^2. It is hence possible to relate the dynamic values at fairlead to the touchdown by

$$\mathbf{Q}_N = \bar{\mathbf{C}}_{N\text{-}1,1}\mathbf{Q}_1 + \bar{\mathbf{D}}_{N\text{-}1,1} \tag{6}$$

where

$$\begin{aligned} \bar{\mathbf{C}}_{n,1} &= \prod_{i=1}^{n} \mathbf{C}_{n-i+1} \\ \bar{\mathbf{D}}_{n,1} &= \begin{cases} \prod_{i=2}^{n}\left(\mathbf{C}_i\bar{\mathbf{D}}_{i-1,1} + \mathbf{D}_i\right) & n > 1 \\ \mathbf{D}_1 & n = 1 \end{cases} \\ \mathbf{C}_i &= \left[\mathbf{I} - \mathbf{A}_{i+1}\frac{\Delta s}{2}\right]^{-1}\left[\mathbf{I} + \mathbf{A}_i\frac{\Delta s}{2}\right] \\ \mathbf{D}_i &= \left[\mathbf{I} - \mathbf{A}_{i+1}\frac{\Delta s}{2}\right]^{-1}\left[\mathbf{B}_{i+1} + \mathbf{B}_i\right]\frac{\Delta s}{2} \end{aligned} \tag{7}$$

which can be further divided into two matrix equations

$$\mathbf{U}_N = \mathbf{c_{11}}\mathbf{U}_1 + \mathbf{c_{12}}\mathbf{T}_1 + \mathbf{d_1} \tag{8}$$

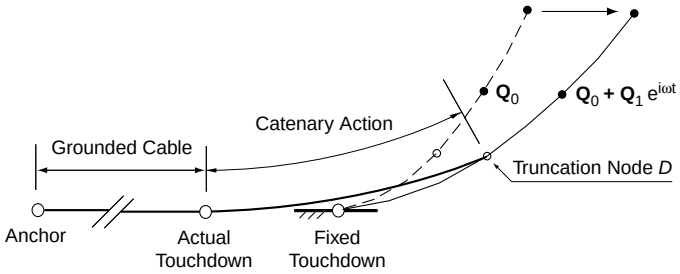

Figure 3. Schematic representation of catenary action at seabed

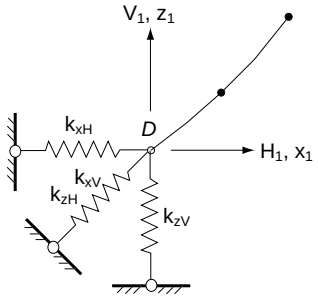

Figure 4. Modelling of seabed interaction with linear springs

$$\mathbf{T}_N = \mathbf{c_{21}}\mathbf{U}_1 + \mathbf{c_{22}}\mathbf{T}_1 + \mathbf{d_2} \tag{9}$$

where $\mathbf{U} = [u_1 \;\; v_1]$, $\mathbf{T} = [T_{e1} \;\; \phi_1]$, $\mathbf{c_{i,j}}$ is the 2-by-2 sub-matrix of $\bar{\mathbf{C}}_{N\text{-}1,1}$, $\mathbf{d_i}$ the 2-by-1 sub-matrix of $\bar{\mathbf{D}}_{N\text{-}1,1}$, and the subscripts N and 1 denote the respective nodes.

As it is conventionally assumed that the touchdown of a mooring cable is pinned at its static position and the motion prescribed at the fairlead, i.e. $\mathbf{U}_1 = 0$ and $\mathbf{U}_N$ is known, the remaining two unknowns, $\mathbf{T}_N$ and $\mathbf{T}_1$, can be obtained easily from Eqs. (8) and (9).

SEABED INTERACTION

When a cable undergoes excitation, a section of the cable measuring from the anchor to the touchdown interacts with the seabed. This interaction, schematically represented in Fig. 3, can be sub-divided into two distinct actions—(i) the axial stretching of the cable lying on the seabed which we call *grounded cable*, and (ii) the liftoff-and-touchdown behaviour which we call *catenary action*. To model this interaction, we truncate the static cable at an arbitrary node D near the static touchdown and replace it with a system of equivalent linear springs shown in Fig. 4.

Since node D is now free i.e. $\mathbf{U}_D \neq 0$, we have three unknowns and require one more equation. The third equation can be derived from the linear springs at D by relating the dynamic component forces at D to their respective dynamic displacements

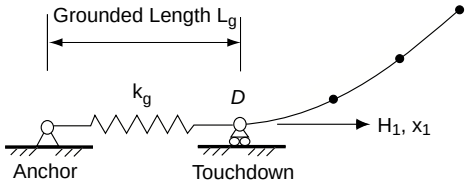

Figure 5. Modelling of grounded cable with a linear spring

$$\begin{bmatrix} V_1 \\ H_1 \end{bmatrix} = \begin{bmatrix} k_{zV} & k_{xV} \\ k_{zH} & k_{xH} \end{bmatrix} \begin{bmatrix} z_1 \\ x_1 \end{bmatrix} \tag{10}$$

where $k_{zV}, k_{xV}, k_{zH}, k_{xH}$ each denotes the stiffness of the respective springs. Similarly, z_1 and x_1 are related to u_1 and v_1 by

$$\begin{bmatrix} z_1 \\ x_1 \end{bmatrix} = \frac{1}{i\omega} \begin{bmatrix} \sin\phi_0 & \cos\phi_0 \\ \cos\phi_0 & -\sin\phi_0 \end{bmatrix} \begin{bmatrix} u_1 \\ v_1 \end{bmatrix} \tag{11}$$

and the force components V_1 and H_1 to T_{e1} and ϕ_1 in the original formulation by

$$\begin{bmatrix} V_1 \\ H_1 \end{bmatrix} = \begin{bmatrix} \sin\phi_0 & T_{e0}\cos\phi_0 \\ \cos\phi_0 & -T_{e0}\sin\phi_0 \end{bmatrix} \begin{bmatrix} T_{e1} \\ \phi_1 \end{bmatrix} \tag{12}$$

The third equation required to relate $\mathbf{T}_D$ to $\mathbf{U}_D$ at node D can thus be found by combining Eqs. (10), (11) and (12), which can then be substituted into Eqs. (8) and (9) to solve for $\mathbf{T}_N$.

Grounded Cable

The axial stretching of the cable lying on the seabed is usually modelled by a linear spring [2–4] attached horizontally to the suspended cable at the static touchdown, as shown in Fig. 5.

Ignoring any catenary action and the friction between cable and seabed, we have

$$\begin{bmatrix} k_{zV} & k_{xV} \\ k_{zH} & k_{xH} \end{bmatrix} = \begin{bmatrix} 0 & 0 \\ 0 & k_g \end{bmatrix} \quad \text{where} \quad k_g = \frac{AE}{L_g} \tag{13}$$

Catenary Action

The liftoff and touchdown behaviour of the cable can be approximated by replacing the truncated dynamic cable with a static catenary between node D and the anchor, see Fig. 6. It is assumed that the effects of fluid drag and inertia on this section of cable are relatively small and therefore can be ignored. Rather than solving for the actual cable at D, the static catenary

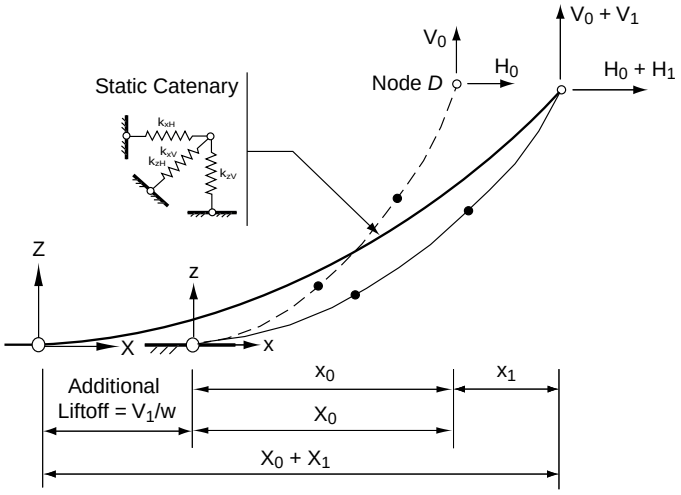

Figure 6. Closeup view of point D near seabed

is approximated by a system of linear springs, whose stiffnesses are determined from either full or linearised catenary equations. Presently, any impact forces arising from the catenary action [9, 10] are ignored.

Full Catenary. Closed form catenary equations can be obtained by assuming the cable is pinned and horizontal at touchdown, i.e. $z = x = \phi = 0$ when $s = 0$, and no fluid drag. Hence, the horizontal and vertical coordinates of the catenary are

$$Z = \frac{H}{w}\left[\sqrt{\left(\frac{V}{H}\right)^2 + 1} - 1\right] + \frac{V^2}{2wAE} \tag{14}$$

$$X = \frac{H}{w}\left[\sinh^{-1}\left(\frac{V}{H}\right) + \frac{V}{AE}\right] \tag{15}$$

where X is measured from the *instantaneous* touchdown of the static cable, and which can be converted to the local coordinate of x_0 measured instead from the *fixed* static touchdown. Taking into account the extension of the grounded cable due to H_1, we can relate the local coordinates to the global system by $x_1 = X_1 - V_1/w + H_1/k_g$, as illustrated in Fig. 6. Note that the last term in the expression for x_1 is due to the axial stretching of the grounded cable mentioned earlier.

Linearised Catenary. The above catenary equations are nonlinear and will therefore have to be linearised for the scheme to be adopted into the frequency domain analysis. The linearisation will "transform" the catenary relationship into the system of linear springs described above.

To do this, we first express the catenary equations as cubic polynomials using Taylor's expansion, thus rewriting Eqs. (14) and (15) as

$$\begin{aligned} z_1 = {} & g_1 H_1 + g_2 V_1 + \\ & g_3 H_1^2 + g_4 H_1 V_1 + g_5 V_1^2 + \\ & g_6 H_1^3 + g_7 H_1^2 V_1 + g_8 H_1 V_1^2 + g_9 V_1^3 \end{aligned} \tag{16}$$

$$\begin{aligned} x_1 = {} & (f_1 + 1/k_g) H_1 + (f_2 - 1/w) V_1 + \\ & f_3 H_1^2 + f_4 H_1 V_1 + f_5 V_1^2 + \\ & f_6 H_1^3 + f_7 H_1^2 V_1 + f_8 H_1 V_1^2 + f_9 V_1^3 \end{aligned} \tag{17}$$

where the Taylor's coefficients g_i and f_i are

$$\begin{aligned} g_1 &= \frac{1}{w}(\cos\phi_0 - 1) \\ g_2 &= \frac{1}{w}\left(\sin\phi_0 + \frac{V_0}{AE}\right) \\ g_3 &= \frac{V_0}{2wH_0^2}(\sin\phi_0 - \sin^3\phi_0) \\ g_4 &= -\frac{1}{wH_0}(\sin\phi_0 - \sin^3\phi_0) \\ g_5 &= \frac{1}{2wV_0}\left(\sin\phi_0 - \sin^3\phi_0 + \frac{V_0}{AE}\right) \\ g_6 &= -\frac{V_0}{2wH_0^3}\left(\sin\phi_0 - 2\sin^3\phi_0 + \sin^5\phi_0\right) \\ g_7 &= \frac{1}{2wH_0^2}\left(2\sin\phi_0 - 5\sin^3\phi_0 + 3\sin^5\phi_0\right) \\ g_8 &= -\frac{1}{2wH_0V_0}\left(\sin\phi_0 - 4\sin^3\phi_0 + 3\sin^5\phi_0\right) \\ g_9 &= -\frac{1}{2wV_0^2}\left(\sin^3\phi_0 - \sin^5\phi_0\right) \\ f_1 &= \frac{1}{w}\left[\sinh^{-1}\left(\frac{V_0}{H_0}\right) - \sin\phi_0 + \frac{V_0}{AE}\right] \\ f_2 &= \frac{1}{w}\left(\cos\phi_0 + \frac{H_0}{AE}\right) \\ f_3 &= -\frac{1}{2wH_0}\sin^3\phi_0 \\ f_4 &= \frac{1}{w}\left(\frac{1}{AE} + \frac{1}{V_0}\sin^3\phi_0\right) \\ f_5 &= -\frac{H_0}{2wV_0^2}\sin^3\phi_0 \\ f_6 &= \frac{1}{6wH_0^2}\left(4\sin^3\phi_0 - 3\sin^5\phi_0\right) \\ f_7 &= -\frac{3}{2wV_0H_0}\left(\sin^3\phi_0 - \sin^5\phi_0\right) \end{aligned} \tag{18}$$

$$f_8 = \frac{1}{2wV_0^2}\left(2\sin^3\phi_0 - 3\sin^5\phi_0\right)$$
$$f_9 = -\frac{H_0}{6wV_0^3}\left(\sin^3\phi_0 - 3\sin^5\phi_0\right)$$

Preliminary tests have shown that the expansion to the power of cubic is sufficiently accurate when compared to the original catenary equations. These polynomials are then linearised to yield a set of closed form linear equations which would otherwise not be easily obtained from the full catenary equations.

Suppose the cubic expressions of z_1 and x_1 can be linearised into a system of linear equations expressed in a matrix form as

$$\begin{bmatrix} z_1 \\ x_1 \end{bmatrix} = \begin{bmatrix} e_{11} & e_{12} \\ e_{21} & e_{22} \end{bmatrix} \begin{bmatrix} V_1 \\ H_1 \end{bmatrix} \tag{19}$$

The required spring stiffnesses at D can therefore obtained inversely by

$$\begin{bmatrix} k_{zV} & k_{xV} \\ k_{zH} & k_{xH} \end{bmatrix} = (e_{11}e_{22} - e_{12}e_{21})^{-1} \begin{bmatrix} e_{22} & -e_{12} \\ -e_{21} & e_{11} \end{bmatrix} \tag{20}$$

In the case of regular wave excitation, we linearise z_1 and x_1 by minimising the square of the residual error over a period—the same method adopted in the linearisation of Morrison's drag [14]. Therefore, to determine e_{11} and e_{12}, we must satisfy

$$\frac{\partial}{\partial e_{11}} \int_0^{\frac{2\pi}{\omega}} E_z^2 \, dt = \frac{\partial}{\partial e_{12}} \int_0^{\frac{2\pi}{\omega}} E_z^2 \, dt = 0 \tag{21}$$

and to determine e_{21} and e_{22}, we must satisfy

$$\frac{\partial}{\partial e_{21}} \int_0^{\frac{2\pi}{\omega}} E_x^2 \, dt = \frac{\partial}{\partial e_{22}} \int_0^{\frac{2\pi}{\omega}} E_x^2 \, dt = 0 \tag{22}$$

where $E_z = z_1 - e_{11}V_1 - e_{12}H_1$ and $E_x = x_1 - e_{21}V_1 - e_{22}H_1$ are the residual errors.

Substituting the complex notation of V_1 and H_1 as $V_1 = |V|\cos(\omega t + \phi_V)$ and $H_1 = |H|\cos(\omega t + \phi_H)$, we obtain the following solutions

$$e_{11} = \frac{h_1A_2 - h_2A_1}{(h_1h_3 - h_2^2)|V|} \tag{23}$$

$$e_{12} = \frac{h_3A_1 - h_2A_2}{(h_1h_3 - h_2^2)|H|} \tag{24}$$

$$e_{21} = \frac{h_1A_4 - h_2A_3}{(h_1h_3 - h_2^2)|V|} \tag{25}$$

$$e_{22} = \frac{h_3A_3 - h_2A_4}{(h_1h_3 - h_2^2)|H|} \tag{26}$$

where

$$\begin{aligned}
A_1 &= g_1h_1|H| + g_2h_2|V| + \\
&\quad g_3h_4|H|^2 + g_4h_5|H||V| + g_5h_6|V|^2 + \\
&\quad g_6h_8|H|^3 + g_7h_9|H|^2|V| + g_8h_{10}|H||V|^2 + g_9h_{11}|V|^3 \\
A_2 &= g_1h_2|H| + g_2h_3|V| + \\
&\quad g_3h_5|H|^2 + g_4h_6|H||V| + g_5h_7|V|^2 + \\
&\quad g_6h_9|H|^3 + g_7h_{10}|H|^2|V| + g_8h_{11}|H||V|^2 + g_9h_{12}|V|^3 \\
A_3 &= (f_1 - k_g)h_1|H| + (f_2 - 1/w)h_2|V| + \\
&\quad f_3h_4|H|^2 + f_4h_5|H||V| + f_5h_6|V|^2 + \\
&\quad f_6h_8|H|^3 + f_7h_9|H|^2|V| + f_8h_{10}|H||V|^2 + f_9h_{11}|V|^3 \\
A_4 &= (f_1 - k_g)h_2|H| + (f_2 - 1/w)h_3|V| + \\
&\quad f_3h_5|H|^2 + f_4h_6|H||V| + f_5h_7|V|^2 + \\
&\quad f_6h_9|H|^3 + f_7h_{10}|H|^2|V| + f_8h_{11}|H||V|^2 + f_9h_{12}|V|^3
\end{aligned} \tag{27}$$

and h_i are integrals of cosines over a period

$$\begin{aligned}
h_1,\, h_3 &= \pi \\
h_2 &= \frac{1}{2}\left[(\pi - 2)\cos 2(\phi_H - \phi_V) + \pi + 2\right] \\
h_4,\, h_7 &= \frac{8}{3} \\
h_5,\, h_6 &= \frac{2}{3}\left[\cos 2(\phi_H - \phi_V) + 3\right] \\
h_8,\, h_{12} &= \frac{3\pi}{4} \\
h_9,\, h_{11} &= \frac{1}{8}\left[(3\pi - 4)\cos 2(\phi_H - \phi_V) + 3\pi + 4\right] \\
h_{10} &= \frac{\pi}{4}\left[\cos 2(\phi_H - \phi_V) + 2\right]
\end{aligned} \tag{28}$$

The entire scheme must be solved iteratively until all the coefficients e_{ij} converge. Once the e_{ij}'s are established, the required spring stiffnesses can be obtained easily from Eq. (20).

Further consideration must be given to the location of truncation node D. If node D is located too high up in the cable, too much dynamic cable will be lost thus forfeiting the purpose. Ideally, the location of D must always lie above the seabed but yet as close as possible to the seabed. This can be determined by first carrying out a preliminary analysis of the cable with the ground spring k_g and then deciding on a node that always lies above the seabed over a period of excitation.

RESULTS AND VALIDATION

The proposed seabed interaction models are programmed in MATLAB [15] and compared to non-linear time domain analyses carried out in Orcaflex [16].

Test Data		Units	Cable 6	Cable 7
Line type	-	-	Chain	Wire
Cable diameter	d	m	0.140	0.130
Submerged weight	w	kN/m	3.2020	0.6644
Axial stiffness	AE	kN	1.69E6	1.30E6
Dry mass	m_0	kg/m	365.6	81.7
Added mass	m_a	kg/m	25.3	13.6
Normal drag coeff.	C_N	-	3.2	1.8
Tangential drag coeff.	C_T	-	0.6	0.2
Water depth	h	m	82.5	500
Mean fairlead tension	T_f	kN	688	2268
Total length	L	m	711	4000

Table 1. Properties of test cables

Two test cables, taken from a comparative study on the dynamic analysis of moorings initiated by the International Ship and Offshore Structures Congress Committee I2 [17] and detailed in Table 1, are selected for the exercise. Cable 6 represents a chain mooring in shallow waters while Cable 7 a wire mooring in deep waters. These conditions generally reflect the usage of the two line types in different water depths. The horizontal offsets given in the paper [17] are already taken into account in the mean fairlead tensions.

The cables are further divided into six different configurations, detailed in Table 2 and shown in Fig. 7, to examine the effect of seabed interaction and compare results obtained from quasi-static, frequency and time domain analyses.

The cables are excited at the fairlead by a horizontal excitation of 1m over wave periods of 4s to 40s. For simplicity, the cable is assumed to be in still water with no wave current or wave excitation, i.e. $V_c = A_w = 0$. These additional effects can be easily included once the proposed model has shown to work. For Model E, the truncation node D for Cable 6 and 7 are chosen at 7.3m and 76.9m (both at 4.3% of the total suspended length) respectively from the initial static touchdown.

Figures 8 and 9 show the dynamic amplifications of fairlead tension for different models. The results show that the effect of seabed interaction is more profound for Cable 7 than Cable 6. For Cable 6, the amplification remains the same for any configurations, proving there is little stretching of the grounded cable or catenary action. In this case, analysing the cable as pinned provides accurate results. For Cable 7, significant reduction in tensions can be seen in Models A, D and E where seabed interaction is included. Furthermore, it is observed that the modelling

Model	Description
A	Time domain simulations in Orcaflex: • Cable pinned at anchor • Grounded cable present • Seabed flat and frictionless
B	Time domain simulations in Orcaflex: • Cable pinned at static touchdown • Grounded cable absent • Seabed absent
C	Frequency domain simulations in MATLAB: • Cable pinned at static touchdown • Grounded cable absent • Seabed absent
D	Frequency domain simulations in MATLAB: • Cable truncated at static touchdown • Grounded cable modelled with ground spring • Catenary action ignored
E	Frequency domain simulations in MATLAB: • Cable truncated at node D • Grounded cable modelled with linearised catenary • Catenary action modelled with linearised catenary
F	Quasi-static simulations in MATLAB: • Cable pinned at instantaneous touchdown • Grounded cable absent • Catenary action modelled implicitly

Table 2. Description of various cable analyses

of the grounded cable alone in Model D produces sufficiently accurate results compared to time-domain simulations of Model A. The linearised catenary in Model E has little effect but nevertheless also produces equally accurate results. Note that there is no dynamic amplification for Model F since it is based purely on a static calculation.

For both cables, catenary action appears to be less important than stretching of the grounded cable. Both Models D and E of Cables 6 and 7 produce very similar and accurate results. This is because both cables have been excited by a fairly small excitation of 1m, leading to catenary actions that are hardly noticeable. Stretching of the cable has become more important than catenary action in this case.

The effect of catenary action becomes more prominent when the amplitude of excitation increases. Figures 10 and 11 show the dynamic amplifications of Cables 6 and 7 in 10s excitation for an amplitude of up to 10m. The results from Model B are not shown here because the dynamic amplification due to the touchdown being pinned are unrealistically large.

From Fig. 10, it can be deduced that although Cable 6 ex-

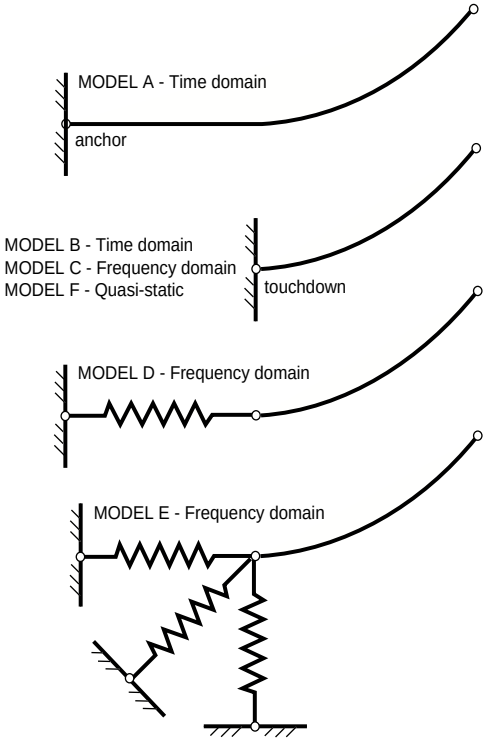

Figure 7. Cable configurations of Models A to F

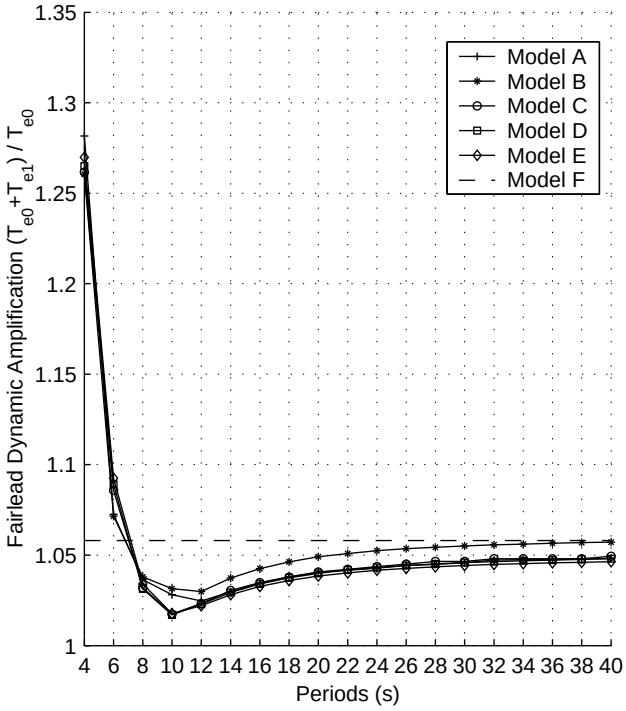

Figure 8. Fairlead dynamic amplification of Cable 6 at 1m excitation

hibits little stretching of the grounded cable, as discovered earlier, the effect of catenary action becomes more profound with increasing excitation. As excitation increases, the results from Model C and D where catenary action is not modelled begin to deviate from the time domain solution of Model A. In this case, the linearised catenary system implemented in Model E produced better results.

For Cable 7, Models D and E both produce very similar and accurate results, demonstrating again the more dominant effect of grounded cable over catenary action. We also see that the assumption of a pinned touchdown in Model C produces erroneous results. For both cables, the static solutions of Model F have become unreliable, especially in Cable 7.

To further investigate the effect of catenary action, Cable 6 is reanalysed under pretensions of 400kN to 4000kN in 10m 10s excitation. As a result of larger displacements near the seabed, the truncation point of Cable 6 in Model E was also repositioned at 16.4% of the total suspended length. The profiles of the cable under various pretensions are shown in Fig. 12.

Figure 13 shows the dynamic amplification of Cable 6 under various pretensions. For pretensions under 2000kN, Model E gives more accurate results than Model D, proving that catenary action is more dominant. As pretension increases beyond 2000kN, the effect of catenary action diminishes and is taken over by the stretching of grounded cable in Model D. At this point, the situation in Cable 6 becomes similar to that of Cable 7 where the excitation of 10m is relatively small in comparison with the total suspended length, thus catenary action has little effect on the fairlead.

On the whole, the variation in dynamic amplification of Model E compares well with that of Model A. However, the tensions in Model E are always lower than that of D because a section of the dynamic cable has been replaced by springs which ignore fluid drag and dynamic effects. Again, the same conclusion can be drawn for Model C where pinning the cable at touchdown produces erroneous results.

CONCLUSIONS

By resolving seabed interaction into two primary actions—(i) axial stretching of grounded cable and (ii) catenary action at touchdown, we have shown that it is possible to model each action with a system of linear springs.

The following principal conclusions can be drawn from this study:

1. Seabed interaction is important even for cables under small excitation. Pinning the cable at touchdown can lead to erroneous results.
2. For cables under low pretensions, catenary action is important and can be modelled using the proposed linearised catenary method.

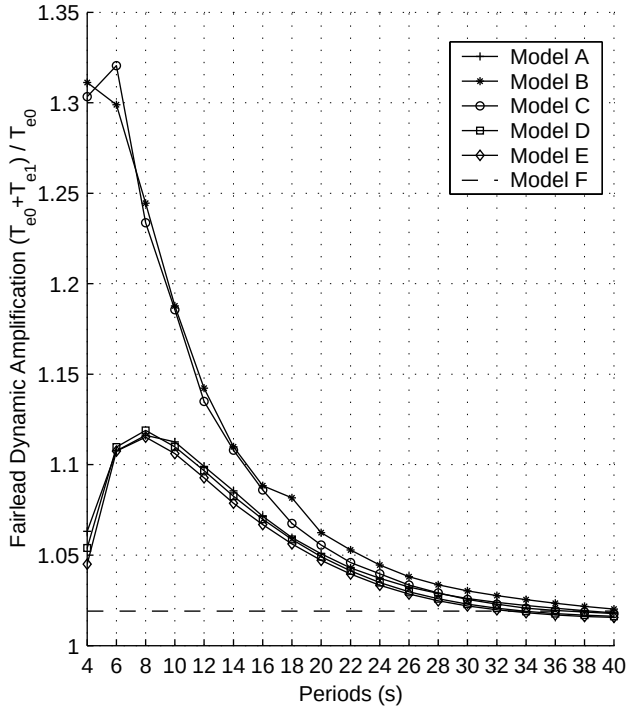

Figure 9. Fairlead dynamic amplification of Cable 7 at 1m excitation

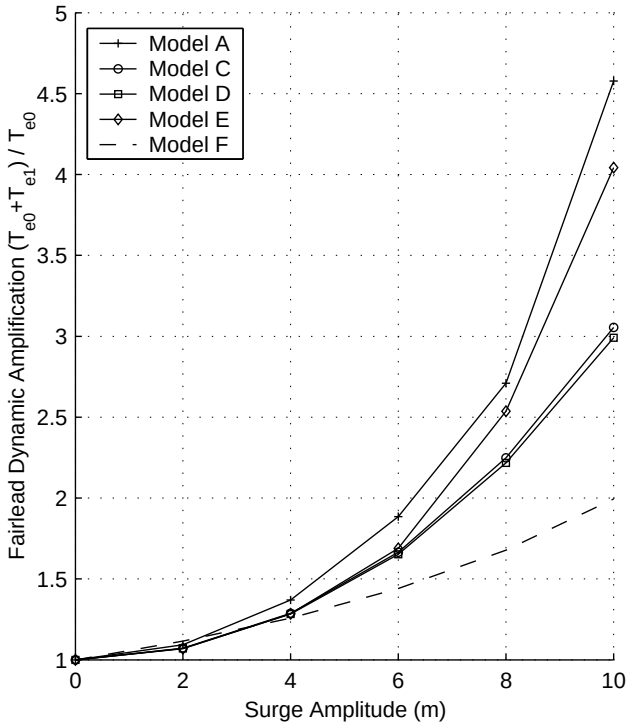

Figure 10. Fairlead dynamic amplification of Cable 6 at 10s excitation

3. For cables under high pretensions, the stretching effect of grounded cable becomes more important and modelling of this effect alone with an equivalent linear spring will suffice.

The proposed method of modelling liftoff and touchdown of the cable using a system of linearised springs has been shown to work well in two test cases. In other cases, modelling the stretching of grounded cable alone with a horizontal spring will suffice. Whether to adopt the former or latter will depend on the cable configuration. In general, the combination of both methods will yield results in reasonable agreement with time domain simulations, as we have shown.

ACKNOWLEDGMENT

The authors wish to thank Dr R. V. Ahilan and Dr Xiao-Ming Cheng of Noble Denton Europe, Dr Brian Corr of BP Amoco, and Prof R. S. Langley of University of Cambridge for their contributions and advice. Helpful comments on the presentation of this paper by anonymous referees are also gratefully acknowledged. Lastly, the authors are indebted to the Department of Trade and Industry and BP Amoco for their financial support.

REFERENCES

[1] Goodman, T. R., and Breslin, J. P., 1976, Statics and dynamics of anchoring cables in waves, *J Hydronautics*, **10**(4):113–120.

[2] Mavrakos, S. A., Papazoglou, V. J., Triantafyllou, M. S., and Hatjigeorgiou, J., 1996, Deep water mooring dynamics, *Marine Structures*, **9**:181–209.

[3] Kwan, C. T., and Bruen, F. J., 1991, Mooring line dynamics - comparison of time domain, frequency domain, and quasi-static analyses, *Offshore Tech Conf*, (6657):95–108.

[4] Wu, S., 1999, Investigation into three mooring line - seabed interaction models for frequency-domain mooring line dynamic analysis, *Proc 9th Int Offshore and Polar Eng Conf*, 320–325.

[5] Chatjigeorgiou, I. K., and Mavrakos, S. A., 1998, Assessment of bottom-cable interaction effects on mooring line dynamics, *Int Offshore Mech and Arctic Eng Conf*, 355.

[6] Ghadimi, R., 1998, A simple and efficient algorithm for the static and dynamic analysis of flexible marine risers, *Computers and Structures*, **29**(4):541–555.

[7] Inoue, Y., and Surendran, S., 1994, Dynamics of the interaction of mooring line with the sea bed, *Proc 4th Int Soc Offshore and Polar Eng*, **2**:317–323.

[8] Webster, W. C., 1995, Mooring-induced damping, *Ocean Eng*, **22**(6):571–591.

[9] Triantafyllou, M. S., Bliek, A., and Shin, H., 1985, Dynamic analysis as a tool for open-sea mooring system design, *Trans SNAME*, **93**:303–324.

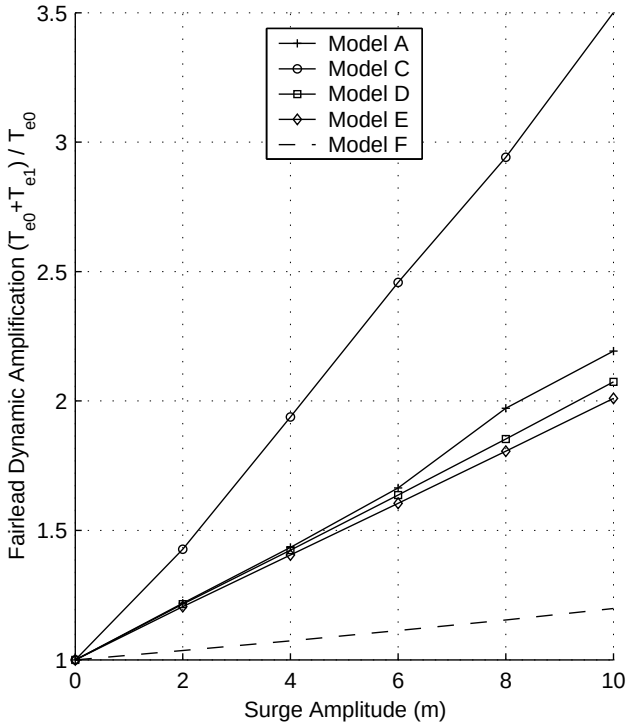

Figure 11. Fairlead dynamic amplification of Cable 7 at 10s excitation

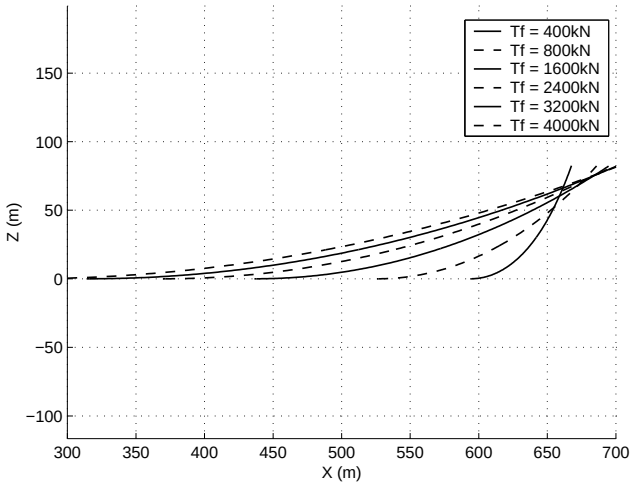

Figure 12. Profile of Cable 6 under various fairlead pretensions T_f

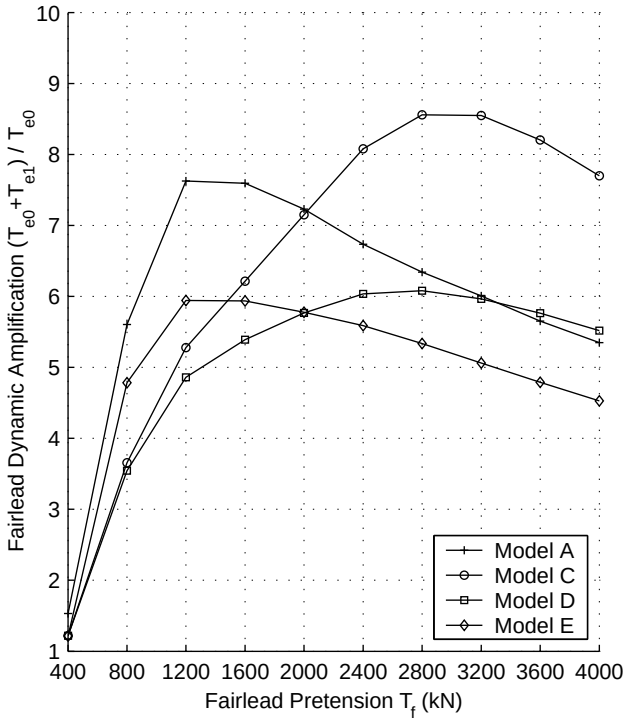

Figure 13. Fairlead dynamic amplification of Cable 6 at 10m 10s excitation

linearization technique for frequency domain riser analysis, *Offshore Tech Conf*, (3777):341–353.

[13] Bliek, A., 1984, *Dynamic Analysis of Single Span Cables*, PhD thesis, Massachusetts Institute of Technology.

[14] Shin, H., 1985, *Numerical solution of the cable dynamic equations using the linearized equivalent damping force*, Master's thesis, Massachusetts Institute of Technology.

[15] MathWorks, 2001, MATLAB *6 Student Version Release 12*, The MathsWorks Inc.

[16] Orcina, 2001, *Visual Orcaflex 7.5 User Manual*, Orcina Ltd, Cumbria, First edition.

[17] Brown, D. T., and Mavrakos, S., 1999, Comparative study on mooring line dynamic loading, *Marine Structures*, **12**:131–151.

[10] Gobat, J. I., and Grosenbaugh, M. A., 2001, Dynamics in the touchdown region of catenary moorings, *Int J Offshore and Polar Eng*, **11**(4):273–281.

[11] Thomas, D. O., and Hearn, G. E., 1994, Deepwater mooring line dynamics with emphasis on seabed interference effects, *Offshore Tech Conf*, (7488):203–214.

[12] Krolikowski, L. P., and Gay, T. A., 1980, An improved